Applied Mathematics & Information Sciences
An International Journal

http://dx.doi.org/10.18576/amis/150606

The Finite Bessel Transforms

Kenan Uriostegui and Kurt Bernardo Wolf*

Institute of Physical Sciences, National Autonomous University of México, Morelos 62251, México

Received: 2 Jun. 2021, Revised: 2 Sep. 2021, Accepted: 17 Oct. 2020
Published online: 1 Nov. 2021

Abstract: Special functions that are generated by a Fourier transform over a circle, also provide *discrete* counterparts, where the circle is substituted by N equidistant points over that circle, with the finite Fourier transform over them. This process was applied to Bessel and Mathieu functions in [*Appl. Math. Inf. Sci.* **15**, 307–315 (2021)]. The resulting *discrete Bessel functions*, $B_n^N(x)$, $n \in \{0,1,\ldots,N-1\}$, satisfy the linear and Graf quadratic relations of their continuous counterparts, and provide a very close numerical approximation with $\lim_{N\to\infty} B_n^N(x) = J_n(x)$. In this paper, the $N\times N$ matrices $\mathbf{B} = \|B_{n,m}\|$, for $B_{n,m} := B_n^N(x_m)$ over $x_m \in \{0,1,\ldots,N-1\}$, are used to define transform kernels between N functions of position f_m and of Bessel mode $\widetilde{f}_n$, which are efficient for the Fourier analysis of discrete signals with $f_m \propto m^{-1/2}$ decay.

Keywords: Bessel functions, Fourier analysis, Discrete transforms, Numerical approximation and analysis

1 Introduction: discrete Bessel functions

In Fourier analysis a strategy to approximate a function defined through the Fourier integral transform over a circle by an N-point cyclic finite Fourier transform, is to replace integrals by finite sums over $N := 2j+1$ (j integer or half-integer) equidistant points φ_k on the circle, with

$$\begin{gathered}\frac{1}{2\pi}\int_{-\pi}^{\pi} \mathrm{d}\varphi\, f(\varphi) \longrightarrow \frac{1}{N}\sum_{k=-j}^{j} f(\varphi_k),\\ \varphi \longrightarrow \varphi_k := 2\pi k/N \quad \text{so} \quad \mathrm{d}\varphi \longrightarrow \varphi_{k+1}-\varphi_k = 2\pi/N.\end{gathered} \tag{1}$$

The Bessel functions of the first kind and integer orders $J_n(x)$, are defined by such a Fourier transform [1, Eq. 8.411.1], as

$$J_n(x) := \frac{1}{2\pi}\int_{-\pi}^{\pi} \mathrm{d}\varphi\, \exp(\mathrm{i}x\sin\varphi)\Big[C_n\cos(n\varphi) - \mathrm{i}S_n\sin(n\varphi)\Big],$$

$$\begin{aligned} C_n &:= |\cos(\tfrac12 n\pi)| = \begin{cases} 1, & n \text{ even},\\ 0, & n \text{ odd},\end{cases}\\ S_n &:= |\sin(\tfrac12 n\pi)| = \begin{cases} 0, & n \text{ even},\\ 1, & n \text{ odd}.\end{cases}\end{aligned} \tag{2}$$

In Ref. [2] the authors proposed in this way to discretize the Bessel function from its integral definition to the N-point sum; however, their results were incomplete for not having respected the difference between the even and odd orders, which take values over different sets of points over the circle. Based on (1) and (2) we proposed in [3] that the correct definition of the *discrete Bessel functions* should be

$$\begin{aligned} B_n^N(x_m) &:= \frac{1}{2j+1}\sum_{k=-j}^{j} \exp(\mathrm{i}x_m\sin\varphi_k)\\ &\qquad\times\Big[C_n\cos(n\varphi_k) - \mathrm{i}S_n\sin(n\varphi_k)\Big],\\ &= \frac{1}{2j+1}\sum_{k=-j}^{j} \exp(\mathrm{i}x_m\sin\varphi_k)\begin{cases} \cos n\varphi_k, & n \text{ even},\\ -\mathrm{i}\sin n\varphi_k, & n \text{ odd},\end{cases}\end{aligned} \tag{3}$$

where $n \in \{0,1,\ldots,N-1 = 2j\}$ are integers while x is a real number. Here we shall be interested in using the *integer* values $x_m = m$, whose range we can set to be $m \in \{-j,-j+1,\ldots,j\}$ or $\{0,1,\ldots,N-1 = 2j\}$, due to the symmetries and modularities of the discrete Bessel functions

$$\begin{aligned} B_n^N(m) &= (-1)^n B_{-n}^N(m) = (-1)^m B_n^N(-m),\\ B_{2n}^N(e^{\mathrm{i}\pi k}2m) &= e^{2\mathrm{i}\pi km} B_{2n}^N(2m), \quad B_n^N(0) = \delta_{n,0},\\ B_{2n+1}^N(e^{\mathrm{i}\pi k}(2m+1)) &= e^{(2m+1)\mathrm{i}\pi k} B_{2n+1}^N(2m+1),\end{aligned} \tag{4}$$

$$B_n^N(m) \;=\; B_{n+N}^N(m) = B_n^N(m+N) \quad \text{real}, \tag{5}$$

where the first three lines are directly inherited from the continuous Bessel functions (for k even all phases are

* Corresponding author e-mail: rkuu@icf.unam.mx

unity so the equalities are trivial), while the last line assumes that m is discrete and integer-spaced. In any case, for continuous argument x, it is clear that, for growing N,

$$\lim_{N\to\infty} B_n^N(x) = J_n(x), \tag{6}$$

is a pointwise limit.

Physically, Fourier-Bessel analysis originates from the radial part of two-dimensional Fourier analysis, where solutions of the wave equation in cylindrical coordinates yield the functions known collectively as cylinder functions. Among these, Bessel functions of the first kind and of integer order, $J_n(x)$, are the coefficient functions for a plane wave generating function [1, 8.511.3],

$$\begin{aligned} e^{\mathrm{i}x\sin\varphi} = J_0(x) + 2\sum_{n=1}^{\infty} J_{2n}(x)\cos(2n\varphi) \\ + 2\mathrm{i}\sum_{n=0}^{\infty} J_{2n+1}(x)\sin((2n+1)\varphi), \end{aligned} \tag{7}$$

for $x \in \mathscr{R}$ real and $\varphi \in \mathscr{S}^1$ on the circle. The discrete counterpart for N points over the circle, which is equivalent to (4), can be used to define the discrete Bessel functions $B_n^N(x)$ by their generating function as

$$\begin{aligned} e^{\mathrm{i}x\sin\varphi_k} = B_0^N(x) + 2\sum_{n=1}^{N-1} B_{2n}^N(x)\cos(2n\varphi_k) \\ + 2\mathrm{i}\sum_{n=0}^{N-1} B_{2n+1}^N(x)\sin((2n+1)\varphi_k), \end{aligned} \tag{8}$$

where $x \in \mathscr{R}$ and $\varphi_k = 2\pi k/N \in \mathscr{S}_N^1$, i.e., with plane waves only in the N directions of $\mathscr{S}_N^1$. For instance, $N=3$ discrete Bessel wavefields will exhibit the C_3 plane rotation symmetry of graphene.

In the following Sect. 2 we show that the discrete $B_n^N(m)$ functions exhibit exact counterparts of some properties satisfied by the continuous Bessel functions $J_n(x)$. These include linear relations that we can prove straightforwardly and the quadratic relation known as *Graf's formula* [4] here placed in the Appendix, since they were not explicitly proven in Ref. [3].

Although we should expect that the discrete Bessel functions approximate their continuous counterparts, it is rather surprising to see how closely they do. In Sect. 3 we compare them numerically in a region of the grid of integer indices (n,m). The point-to-point differences between the two in $n=j$ and $0 \le m \le N-1$ are of the order of 10^{-16} for $N > 91$; they are smallest for values of m close to zero.

The $N\times N$-matrix $\mathbf{B}^N = \|B_n^N(x_m)\|$ formed in (4) will be used in Sect. 4 as the kernel that defines the *finite Bessel transform*. This transform is analogous to the finite N-point Fourier transform as approximant to the Fourier (series) transform over the circle. The finite Bessel transform intertwines N-point functions of position $f_m \equiv f(x_m)$ with N Bessel-mode functions $\widetilde{f}_n$.

Discrete analogues of continuous functions have both computational and analytical interest. In the Bessel case, from an early definition in Ref. [5] to recent work based on difference equations, postulated analogues to the differential equation [6,7] have resulted in definitions that are not equivalent to those of Ref. [2] nor to the one we study here. In the concluding Sect. 5 we emphasize that the present discrete analogue and its associated transform are both physically natural and can be numerically useful.

2 Linear and Graf discrete Bessel identities

The discrete Bessel functions $B_n^N(m)$ obey analogues of several well-known identities satisfied by the continuous Bessel functions $J_n(x)$; these were stated without explicit proof in Ref. [3]. For simplicity we shall omit the upper N-index, understanding that $N = 2j+1$, allowing the position coordinate $x_m \equiv m$ to be any real number, and also using the so-called

$$\text{Neumann factor:}\ \ \varepsilon_n := 2-\delta_{n,0} = \begin{cases} 1, & n=0, \\ 2, & n\neq 0. \end{cases} \tag{9}$$

It is then straightforward to use symmetry and covariance relations, (4) and (5), to prove that the sum of even orders of the discrete Bessel functions is

$$\sum_{n=-2j}^{2j} B_{2n}(m) = \sum_{n=0}^{2j} \varepsilon_{2n} B_{2n}(m) = B_0(m) + 2\sum_{n=1}^{j} B_{2n}(m) = 1, \tag{10}$$

which compare with the corresponding equation in [1, Eq. 8.512.1]. This is a particular case (for $\varphi_k = 0$) of the linear discrete Bessel summations for odd and even orders,

$$\sum_{n=0}^{j} B_{2n+1}(m)\sin((2n+1)\varphi_k) = \tfrac{1}{2}\sin(m\sin\varphi_k), \tag{11}$$

$$\sum_{n=0}^{j} \varepsilon_n B_{2n}(m)\cos(2n\varphi_k) = \cos(m\sin\varphi_k), \tag{12}$$

which are proven, as for the continuous functions, in the four cases of k and n even or odd, using the trigonometric sum identities in [1, Eqs. 1.342.2].

Regarding quadratic expressions, a sum found by Neumann in 1867 for integer orders, and extended by Graf in 1893 to all real orders, has been known since as *Graf's formula* [4, Sec. 7.6.2, Eq. (6)]. Its group-theoretic origin is the linear transformation of spherical harmonics $Y_{\ell,m}(\theta,\phi)$ by Wigner-d functions under rotations around the y-axis, contracted for $\ell \to \infty$ [8]. In that limit both spherical harmonics and Wigner d-functions become Bessel functions, yielding

$$\sum_{n=-\infty}^{\infty} J_n(x) J_{n'-n}(x') = J_{n'}(x+x'). \tag{13}$$

This relation contains the displacement and convolution of arguments and of indices. The discrete Bessel functions $B_n(m)$ in (4) satisfy the corresponding *discrete Graf* formula

$$\sum_{n=-2j}^{2j} B_n(m)\,B_{n'\mp n}(m') = B_{n'}(m \pm m'), \tag{14}$$

for $N = 2j{+}1$. Several related expressions are easy to reach for particular cases, such as

$$\text{for } n' = 0, \quad \sum_{n=0}^{2j} \varepsilon_n B_n(m)\,B_n(m') = B_0(m-m'), \tag{15}$$

$$\text{for } m = m', \quad \sum_{n=-2j}^{2j} B_n(m)\,B_{n'+n}(m) = B_{n'}(0) = \delta_{n',0}. \tag{16}$$

$$n' = 0 \text{ and } m = m', B_0(m)^2 + \sum_{n=1}^{2j} B_n(m)^2 = 1. \tag{17}$$

The proof of this relation is detailed in the Appendix.

3 The discrete-to-continuous approximations

In this section we illustrate the approximate equalities $B_n(m) \cong J_n(m)$ and report the differences in the grid (n,m), with $n \in \{0,1,\ldots,N{-}1\}$ and m real. The graphs presented here include those shown in Ref. [3], plus several new ones that pertain related functions beyond the original set. The merit of the approximation is estimated by the mean quadratic error,

$$\Delta_n^N := \frac{1}{N}\sum_{m=0}^{N-1}\Big(J_n(m) - B_n^N(m)\Big)^2. \tag{18}$$

A discrete system of $N = 2j+1$ points $\{x_m\}_{m=0}^{2j}$ is a space spanned by the basis set of N independent functions $J_n(x_m)$. The graphs in Fig. 1 contain intervals of m beyond $[0,2j]$, and up to $4j = 2N-2$. Good matches between discrete and continuous Bessel values in the grid (n,m) are seen to lie in the first quadrant for $n+m \le 3j$. In the interval $[0,2j]$, the mean square error between the values is $\Delta_n^N < 10^{-16}$ for $j = 18$ and $n \le j$.

To have examples of how the mean square error of the discrete Bessel functions decreases as the number of points N in the approximation increases, we include Fig. 2. In the left-hand plot, we can see that for $j = 18$ the mean square error Δ_n^N in (18) becomes of order 10^{-16}, and for $n = j \approx 50$ the error is of order 10^{-32}. In the right-hand side, the orders n are fixed while the number N of points is increased; the error is then reduced to the order of 10^{-32}.

When we enlist other well known formulas that are valid for continuous Bessel functions, and replace them by their discrete version we also find matches with similar approximations. Among them we find

$$\begin{aligned} 2\textstyle\sum_{n=0}^{j}(-1)^n B_{2n+1}(m) &\cong \sin(m), \\ \textstyle\sum_{n=0}^{j} \varepsilon_n (-1)^n B_{2n}(m) &\cong \cos(m), \end{aligned} \tag{19}$$

that can be compared with [1, Eqs. 8.514.1,2]. We point to the fact that in (19), the argument of sine and cosine is *integer* $m \in \{-j,-j{+}1,\ldots,j\}$. In Fig. 3 we compare the functions of discrete m with the continuous functions of m; mean square errors are of the order $\approx 10^{-6}$. For other expressions, in Fig. 4 we show, for $n = 1$ and $m \in [-j,j]$, the approximations

$$\begin{aligned} \textstyle\sum_{k=0}^{j} B_1(m\cos\varphi_k)\cos\varphi_k &\cong \tfrac{\sin m}{m} =: \operatorname{sinc} m, \\ \textstyle\sum_{k=0}^{j} B_1(m\cos\varphi_k) &\cong \tfrac{1-\cos m}{m} =: \operatorname{cosc} m. \end{aligned} \tag{20}$$

that also hold with a mean square error less than 10^{-6}.

4 The Finite Bessel transform

Bessel functions appear in the expansion of two-dimensional wave functions into plane waves arriving from all directions on a circle. Replacing the Fourier series over the full circle by the finite Fourier transform over N points, restricts the the set of formant plane waves to N of them lying on N discrete, equidistant directions on that circle.

A set of N linearly independent vectors can be used as a basis to define an N-dimensional vector space. Let us introduce an $N \times N$ discrete and finite *Bessel matrix* $\mathbf{B} = \|B_{n,m}\|$, $B_{n,m} := B_n(m)$, where the *orders* n and *positions* m are in the ranges $n,m \in \{0,1,\ldots,N{-}1\}$, both integer and real. The numerical verification that $\det\mathbf{B} \neq 0$ for a range of N's supports the conjecture that the set is linearly independent, so we can assume that the unique inverse matrix $\mathbf{C} := \mathbf{B}^{-1}$ exists.

Thus, given a vector of functions $\mathbf{f} = \|f(x_m)\|$ of N *position* arguments $f(x_m) \equiv f_m$, the matrix $\mathbf{B}$ will transform this into the vector $\widetilde{\mathbf{f}} = \mathbf{Bf}$ of components $\widetilde{f}(n) \equiv \widetilde{f}_n$ of N *Bessel mode* arguments, and the inverse matrix $\mathbf{C}$ will then return the original function of positions,

$$\widetilde{f}_n := \sum_{m=0}^{N-1} B_{n,m} f_m, \quad f_m = \sum_{n=0}^{N-1} C_{m,n}\widetilde{f}_n, \qquad \mathbf{BC} = \mathbf{CB} = \mathbf{1}. \tag{21}$$

The transform function $\widetilde{f}_n$ is the projection of $f(x_m)$ on $B_n(x_m)$ under the natural finite inner product that sums over the N positions,

$$(\mathbf{f}^1, \mathbf{f}^2)_N := \sum_{m=0}^{N-1} f^{1*}(m)\, f^2(m). \tag{22}$$

In Fig. 5 we show the density plot of the transform kernel $\mathbf{B} = \|B_{n,m}\|$ on the (n,m) grid, and of its inverse kernel $\mathbf{C} = \|C_{m,n}\|$. The plot for the kernel $\mathbf{B}$ of course resembles closely similar plots of the Bessel functions $J_n(m)$: it has large diagonal elements, vanishingly small values in the lower-left region, and oscillating $\sim m^{-1/2}$

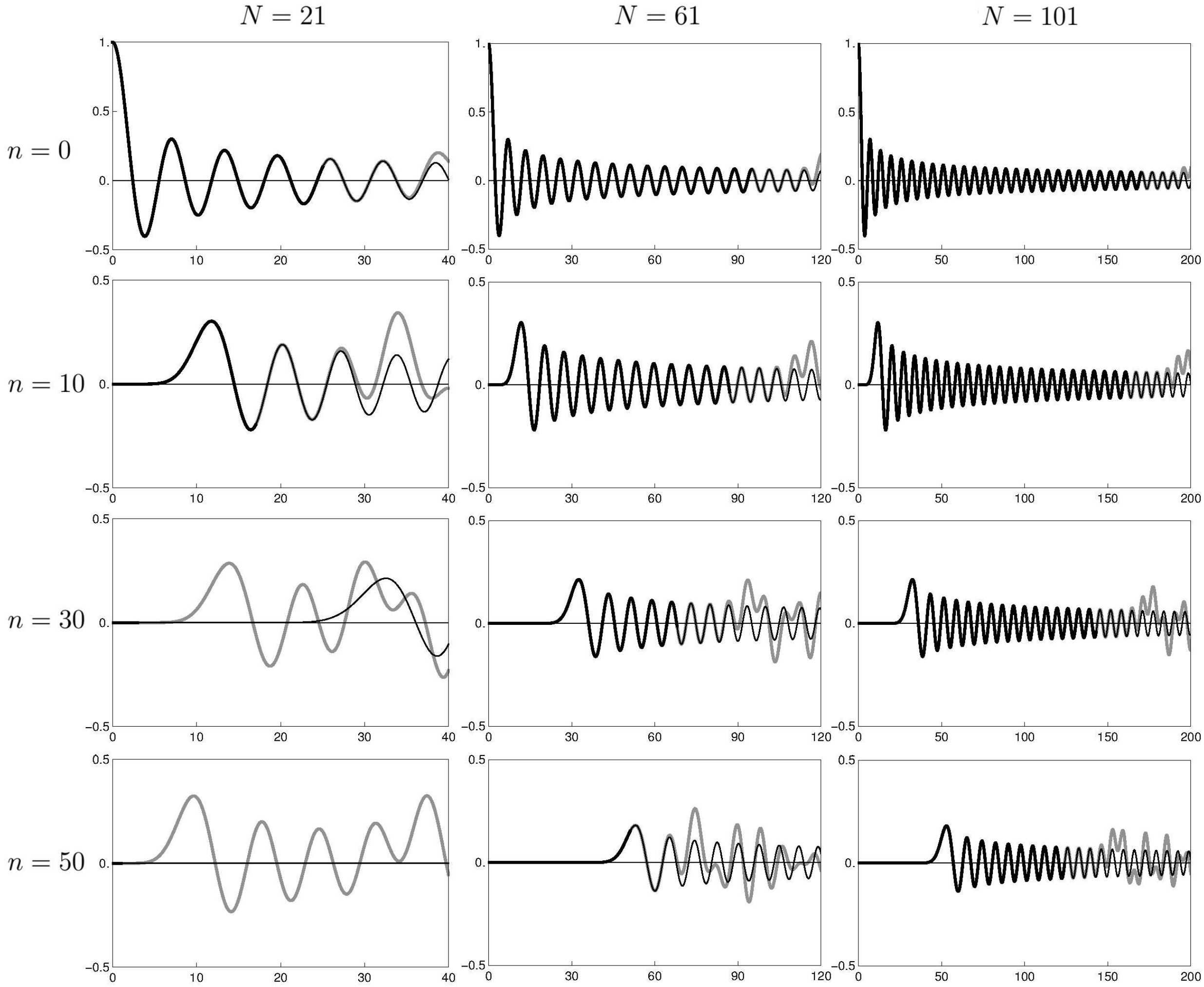

Fig. 1: Comparison of values of the discrete Bessel functions $B_n^{2j+1}(m)$ (open circles) and the continuous Bessel functions $J_n(m)$ (lines) in the same ranges. We show the cases for $j \in \{10, 30, 50\}$, (i.e., $N \in \{21, 61, 101\}$ discrete points), for Bessel orders $n \in \{0, 10, 30, 50\}$, over the argument range $m \in [0, 4j = 2N-2]$. The continuous lines are heavy black where the point-to-point difference between the discrete interpolation and the continuous Bessel values is less than 10^{-16} and replaced by dashed gray lines where it is greater.

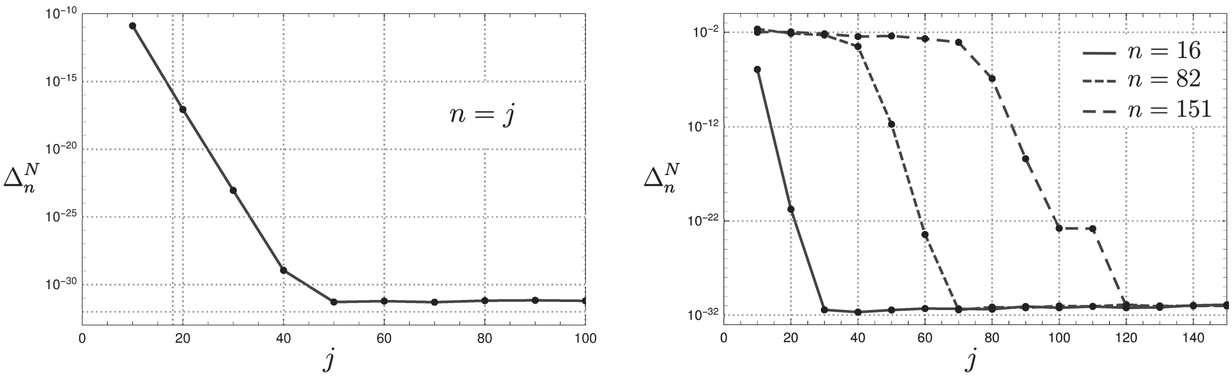

Fig. 2: *Left*: Mean square error Δ_n^N between the discrete and continuous Bessel functions $B_n^N(m)$ for $n = j \in \{10, \ldots, 100\}$. *Right*: The mean square error is reduced for $n \in \{16, 82, 151\}$ as the number of points increases as before.

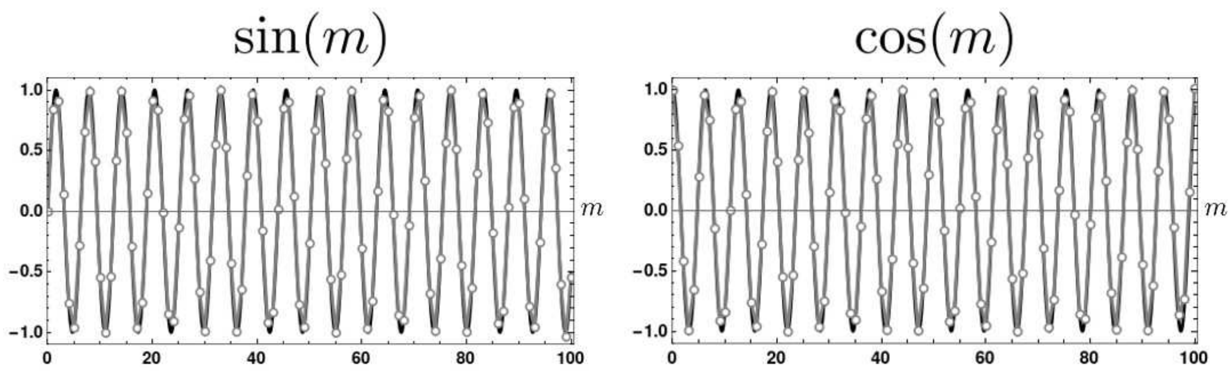

Fig. 3: Comparison of the left-hand sides of Eqs. (19) for integer $m \in [0,100]$ (open circles), and $\sin(m)$ and $\cos(m)$ for continuous m (line) in the same range; here, $j = 50$ and $N = 101$.

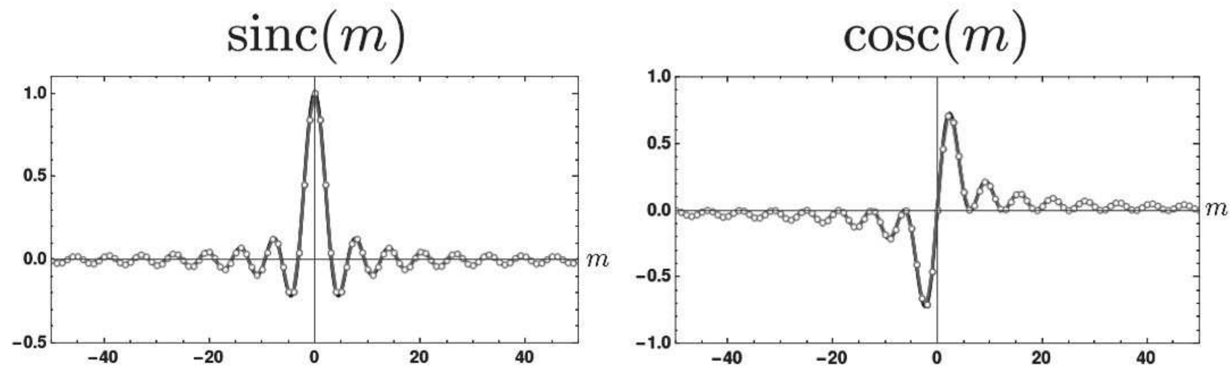

Fig. 4: Comparison of values of the discrete and continuous Bessel functions, left- and right-hands of Eqs. (20), as before with open circles and continuous lines, in the same range for $j = 50$, $N = 101$.

decrease in the upper right part. The determinant of $\mathbf{B}$ is nonzero but it quickly becomes very small: for $N = \{5, 11, 21, 51\}$, we find $\det\mathbf{B} \lesssim \{5.7\times10^{-4}, 2.1\times10^{-18}, 5.3\times10^{-68}, 2\times10^{-288}\}$. Although this does not negate the existence of the finite Bessel transform (21), it will effectively reduce the numerical stability of computations for larger N's, precluding the existence of a proper $N \to \infty$ limit. On the other hand, the inverse transform kernel $\mathbf{C}$ also shown in Fig. 5, does not seem to have a clear structure for which we could surmise an analytic form.

The finite Bessel transform of a Kronecker delta function of positions, $f^{m_\circ}(x_m) = \delta_{m,m_\circ}$, will be a vector of discrete Bessel functions $\widetilde{f}_n = B_n(m_\circ)$ at $m_\circ$. Conversely, the inverse finite Bessel transform of a Kronecker delta of modes, $\widetilde{f}^{n_\circ}_n = \delta_{n,n_\circ}$ will be the vector $B_{n_\circ}(m)$ of discrete Bessel function values of order $n_\circ$. In the continuum, the diffusion of a Dirac delta yields Gaussian bell functions. These Gaussians have several important properties under the Fourier integral transform, chief among them is their self-reproduction with inverse width (see *e.g.* [1, Eq. 6.618.1]) while translations multiply the transform function by a linearly oscillating phase. In Fig. 6 we chose a finite Gaussian function on integer positions, $f_m \sim \exp[-(m-m_\circ)^2/2\omega]$ centered on $m_\circ$ and of width ω. Their finite Bessel transforms, shown in Fig. 6, display roughly the same self-reproduction property of this and other bell-shaped functions, which are real, their maximum corresponding roughly with the top of the original bell; being real, translation of the center of the Gaussian does not lead to phase oscillations as the two functions are and remain real. In that figure we see that the wider the original bell, the smoother its finite Bessel transform, which is also smoother for $m \approx 0$ than for $m \approx N-1$. These results have been validated by numerical experimentation because analytic expressions are not readily available.

The finite Bessel transform $\mathbf{f} \mapsto \widetilde{\mathbf{f}} = \mathbf{B}\mathbf{f}$ is not unitary, nor its inverse. Letting k stand for m or n, their inner

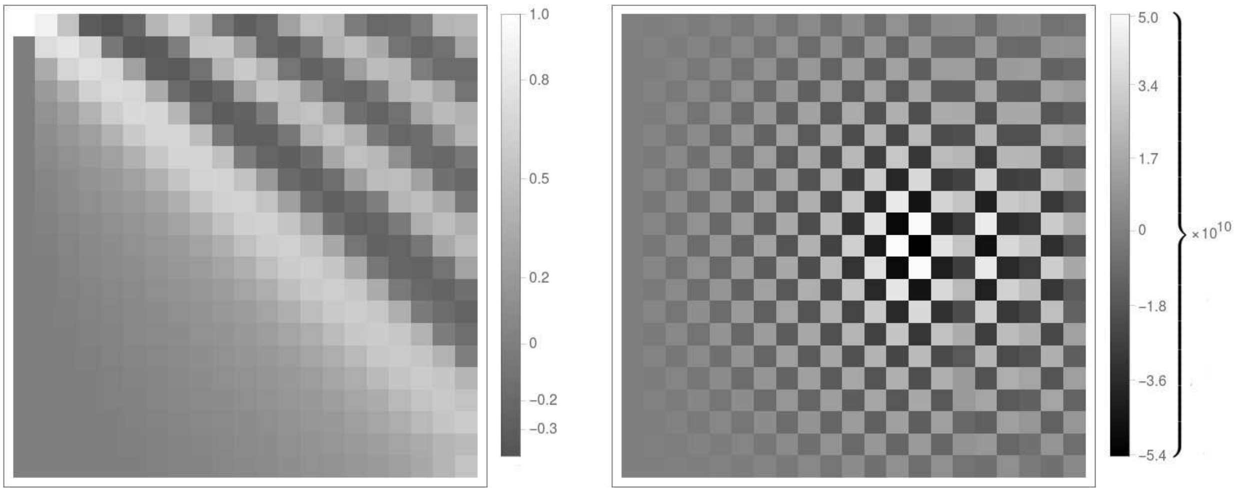

Fig. 5: *Left*: The discrete Bessel elements $B_{n,m}$ of the matrix $\mathbf{B}$, for $N=43$ ($j=21$) closely approximate the values of the Bessel function $J_n(m)$ on the integer grid region $0 \le m,n \le N-1$. Both the continuous and the discrete Bessel functions are small in the lower left $m<n$ triangle, exhibit a maximum around $m \approx n$ with $B_0(0)=1$, and oscillate with decreasing amplitude as $\sim m^{-1/2}$ in the upper-right region $m>n$. *Right*: The inverse finite Bessel transform kernel $\mathbf{C}$ of elements $C_{m,n}$, with gray tones adjusted to the large values of the matrix elements. In both images, the horizontal direction corresponds to the position m and the vertical direction to the order n of the function.

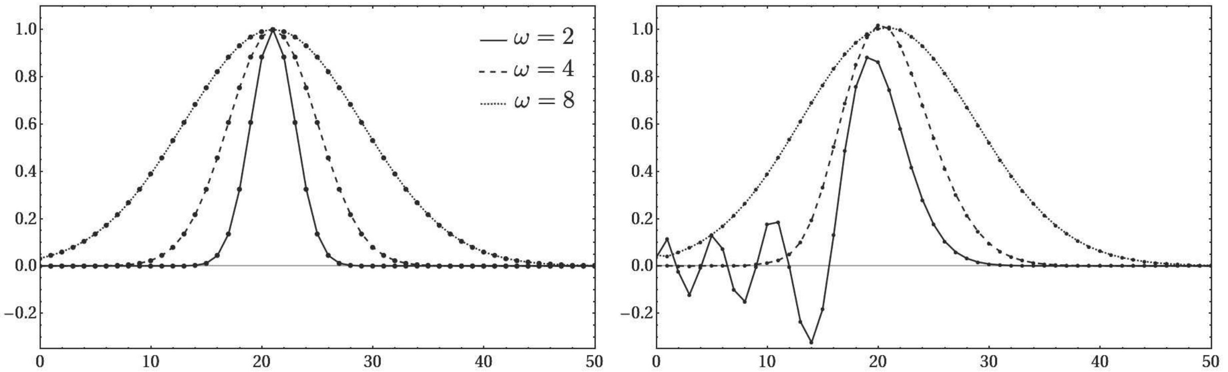

Fig. 6: *Left*: The discrete Gaussian function $\exp[-(m-m_\circ)^2/2\omega]$ for $N=51$ points, centered on $m_\circ=21$ and of widths $\omega=2$, 4 and 8. *Right*: The finite Bessel transforms of these discrete Gaussian functions.

products (22) relate as

$$\sum_{k=0}^{N-1} f_k^{1*} f_{k'}^2 =: (\mathbf{f}^1,\mathbf{f}^2)_N = (\mathbf{C}\widetilde{\mathbf{f}}^1,\mathbf{C}\widetilde{\mathbf{f}}^2)_N = \sum_{k,k'=0}^{N-1} \widetilde{f}_k^{1*} (\mathbf{C}^\dagger\mathbf{C})_{k,k'} \widetilde{f}_{k'}^2. \tag{23}$$

Hence the finite Bessel map can be seen as a unitary transformation from the position space with inner product $(\cdot,\cdot)_N$ in (22) to a second finite space with a nondegenerate metric $\mathbf{C}^\dagger\mathbf{C}$. Convolution also inherits the structure common to all nonsingular transforms: if $\widetilde{\mathbf{f}}^1=\mathbf{B}\mathbf{f}^1$ and $\widetilde{\mathbf{f}}^2=\mathbf{B}\mathbf{f}^2$, then the finite Bessel transform of $f_m := f_m^1 f_m^2$ is

$$\widetilde{f}_n = \sum_{k,k'=0}^{N-1} C_{n;k,k'} \widetilde{f}_k^1 \widetilde{f}_{k'}^2, \quad C_{n;k,k'} := \sum_{m=0}^{N-1} B_{n,m} C_{m,k} C_{m,k'}. \tag{24}$$

Conversely, if $\mathbf{f}^1=\mathbf{B}\widetilde{\mathbf{f}}^1$ and $\mathbf{f}^2=\mathbf{B}\widetilde{\mathbf{f}}^2$, then the finite inverse Bessel transform of $\widetilde{f}_n := \widetilde{f}_n^1 \widetilde{f}_n^2$ is

$$f_m = \sum_{k,k'=0}^{N-1} B_{m;k,k'} f_k^1 f_{k'}^2, \quad B_{m;k,k'} := \sum_{n=0}^{N-1} C_{m,n} B_{k,n} B_{k',n}. \tag{25}$$

This convolution structure is common to the well-known Fourier structure and, extended to other function bases, also encompasses the coupling of angular momenta by Clebsch-Gordan coefficients.

5 Concluding remarks

After trigonometric functions, cylinder —and in particular Bessel— functions can be seen as the most important in mathematical physics. These Bessel functions also have important group-theoretic properties as irreducible representation matrix elements for the Euclidean groups of rotations and translations [9].

Trigonometric functions are the basis for three distinct transforms: the Fourier integral transforms, Fourier series, and the finite Fourier transforms. The three relate through continuous limits and discretizations of the real line $\mathscr{R}$, the integers $\mathscr{Z}$, and on $\mathscr{Z}_N$, the integers modulo N. Such a discretization of the generating functions was used here for $J_n(m)$ on $\mathscr{Z}$ to define $B_n(m)$ on $\mathscr{Z}_N$. As we mentioned before, the position m need not be integer; as occurs in the finite Fourier case, the N phases on the circle can be shifted freely. The values of the discrete Bessel functions in the figures can be similarly defined on an m-line in $[0,N-1]$ or extended beyond. On the other hand, the order n cannot but be integer, because for non-integer $n>0$, $|J_{-n}(0)|$ is infinite.

We may claim, together with Ref. [2], that a probable application of the discrete Bessel functions (4) is the discretization of radial wave propagation with $\sim r^{-1/2}$-decay on scattering in two dimensions, because the basis of discrete Bessel functions $B_n(m)$ has that decrease property. One may expect these to provide a more significant set of mode functions than if the transform used had been the finite Fourier transform, whose oscillation amplitude is constant over the position range.

Finally, we remark that known and named series or integral transforms with kernels involving Bessel functions are quite distinct from the proposed finite Bessel transform in Eqs. (21). The fractional Hankel-n transform kernel [10] contains the factor $\sim (pq)^{1/2} J_n(pq)$, between function spaces $f(q)$ and $\widetilde{f}(p)$; the two-dimensional Fourier-Bessel series with the drum harmonics has the kernel $\sim J_n(k_{n,m}r)\,e^{in\phi}$ in polar coordinates, for integer n,m, and with $k_{n,m}$ being the frequencies allowed by circular and radial boundary conditions. Further series detailed in Watson's treatise [11] are the Neumann-c series with kernel $\sim J_{n+c}(r)$, the Kapteyn-c series with $\sim J_{n+c}((n+c)r)$, and the Schlömlich-c series with $J_n(cr)$, which transform between functions f_n with n integer and $\widetilde{f}_{(c)}(r)$ on continuous r. As can be seen, none of these has the simple structure of the discrete $N\times N$ Bessel matrix that was introduced in Eqs. (21).

Appendix: Proof of the finite Graf summation

To prove the discrete and finite Graf summation formula (14), one can directly replace the discrete functions from (4), respecting the parity and periodicity properties (4) for the N terms in the finite sum, as $\sum_{-j}^{j}$ or $\sum_{0}^{2j}$. The left-hand side of this expression is

$$\sum_{n=-2j}^{2j} B_n(m)\,B_{n'-n}(m') \tag{26}$$
$$= \frac{1}{(2j+1)^2}\sum_{n=-2j}^{2j}\sum_{k,k'=-j}^{j} \exp i(m\sin\varphi_k + m'\sin\varphi_{k'})$$
$$\times\Big[C_{n'-n}\cos((n'-n)\varphi_{k'}) - iS_{n'-n}\sin((n'-n)\varphi_{k'})\Big]$$
$$\times\Big[C_n\cos(n\varphi_k) - iS_n\sin(n\varphi_k)\Big],$$

The sum over n shifts over to the two factors that house the parities in (4), which then separate into two cases, for n' even and n' odd, reconstructing the right-hand side of the discrete Graf formula (14).

For n' even, and n' odd, the sum over n becomes, respectively

$$\sum_{n=-2j}^{2j}\Big[C_nC_{n'-n}\cos(n\varphi_k)\cos((n'-n)\varphi_{k'}) + S_nS_{n'-n}\sin(n\varphi_k)\sin((n'-n)\varphi_{k'})\Big] = (2j+1)\cos(n'\varphi_k)\,\delta_{k,k'}, \tag{27}$$

$$-i\sum_{n=-2j}^{2j}\Big[C_nS_{n'-n}\cos(n\varphi_k)\sin((n'-n)\varphi_{k'}) + S_nC_{n'-n}\sin(n\varphi_k)\cos((n'-n)\varphi_{k'})\Big] = -i\,(2j+1)\sin(n'\varphi_k)\delta_{k,k'}. \tag{28}$$

This brings the left-hand side of (14) closer to $B_{n'}(m+m')$, as

$$\sum_{n=-2j}^{2j} B_n(m)\,B_{n'-n}(m') \tag{29}$$
$$= \frac{1}{2j+1}\sum_{k,k'=-j}^{j} \exp i(m\sin\varphi_k + m'\sin\varphi_{k'})$$
$$\times\Big[\widetilde{C}_{n'}^{k,k'}\cos(n'\varphi_k) - i\widetilde{S}_{n'}^{k,k'}\sin(n'\varphi_k)\Big],$$

where (27) and (28) contribute to the new coefficients

$$\widetilde{C}_{n'}^{k,k'} = \begin{cases} 0, & n' \text{ odd}, \\ \delta_{k,k'}, & n' \text{ even}, \end{cases} \qquad \widetilde{S}_{n'}^{k,k'} = \begin{cases} \delta_{k,k'}, & n' \text{ odd}, \\ 0, & n' \text{ even}. \end{cases} \tag{30}$$

These factors placed in the double sum (26) reduce terms to those with $k=k'$ into a single sum, where the two exponents join to render $(m+m')\sin\varphi_k$, and the left-hand side of (14) has become indeed

$$\frac{1}{2j+1}\sum_{k=-j}^{j}\exp(\mathrm{i}\,(m+m')\sin\varphi_k)\times\Big[C_{n'}\cos(n'\varphi_k)-\mathrm{i}S_{n'}\sin(n'\varphi_k)\Big]=B_{n'}(m+m'). \tag{31}$$

The symmetries (4) indicate that the $4j+1$ summands in $\sum_{n=-2j}^{2j}$ can be reduced to $N=2j+1$ summands by introducing the Neumann factor ε_n in (9), Thus, for $n'=0$ and $m=-m'$, Eq. (14) can be written in the forms

$$\begin{aligned}\textstyle\sum_{n=-2j}^{2j}\Big[B_n(m)\Big]^2 &= \textstyle\sum_{n=0}^{2j}\varepsilon_n\Big[B_n(m)\Big]^2\\ &= \Big[B_0(m)\Big]^2+2\textstyle\sum_1^{2j}\Big[B_n(m)\Big]^2 \qquad (32)\\ &= 1,\end{aligned}$$

that correspond to well-known formulas for Bessel functions with infinite sums. The basic Graf formula that is valid for the discrete Bessel functions yields several of its versions under the symmetries listed in (4). All formulas in Sects. 2 and 3 have been verified numerically for a wide sample of particular cases.

Acknowledgments

We thank the support of the Universidad Nacional Autónoma de México through the PAPIIT-DGAPA AG100119. K.U. acknowledge doctoral fellowship support from CONACyT-México.

Conflict of Interest

The authors declare that they have no conflict of interest.

References

[1] I.S. Gradshteyn and I.M. Ryzhik, *Tables of Integrals, Series and Products*, A. Jeffrey and D. Zwillinger, Academic Press, California USA: 659–958 (2007).
[2] G. Biagetti, P. Crippa, L. Falaschetti, and C. Turchetti, *Discrete Bessel functions for representing the Class of Finite Duration Decaying Sequences*, IEEE 24th 4th European Signal Processing Conference, 2126–2130 (2016).
[3] K. Uriostegui and K.B. Wolf, Discrete Bessel and Mathieu functions, *Appl. Math. Inf. Sci.* **15**, 307–315 (2021).
[4] A. Erdélyi *et al.*, *Higher Transcendental Functions* (Based on notes by H. Bateman) vol. 2, McGraw-Hill, New York USA: 1–78, (1953).
[5] R.H. Boyer, Discrete Bessel functions, *J. Math. Anal. Appl.* **2**, 509–524 (1961).
[6] M. Bohner and T. Cuchta, *The Bessel difference equation*, Proc. Amer. Math. Soc. **145**, 1567–1580 (2017).
[7] A. Slavík, Discrete Bessel functions and partial differential equations, *J. Diff. Eqs. Applics.* **24**, 425–437 (2017).
[8] P. Winternitz, K.B. Wolf, G.S. Pogosyan, and A.N. Sissakian, Graf's addition theorem obtained from SO(3) contraction, *Theor. Mat. Phys.* **129**, 1501–1503 (2001).
[9] J.D. Talman, *Special Functions –A Group Theoretic Approach* (Based on lectures by E.P. Wigner), W.A. Benjamin Inc., New York USA: 198–206, (1968).
[10] M. Moshinsky, T.H. Seligman, and K.B. Wolf, Canonical Transformations and the Radial Oscillator and Coulomb Problems, *J. Math. Phys.* **13**, 901–907 (1972).
[11] G.N. Watson, *Theory of Bessel Functions*, Cambridge University Press, London UK: 14–37, (1922).

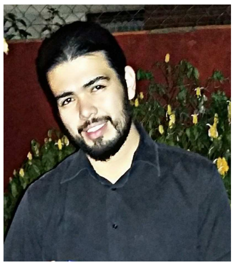

Kenan Uriostegui received the MSc and PhD degree at the Instituto en Ciencias Físicas of the Universidad Nacional Autónoma de México. His main interests include unitary transformations on discrete systems, approximation and numerical analysis, algebraic structures in optomechanical systems and advances in optics and quantum information. He is currently doing postdoctoral research at the Institute of Physics, UNAM under the direction of Dr. C. Pineda.

Kurt Bernardo Wolf is presently Investigador Titular (equivalent to full professor) at the Universidad Nacional Autónoma de México, which he entered in 1971. He was the first director of Centro Internacional de Ciencias A.C. (1986–1994), organizing 14 national and international schools, workshops and conferences. He is author of: Integral Transforms in Science and Engineering (Plenum, New York, 1979) and Geometric Optics on Phase Space (Springer-Verlag, Heidelberg, 2004), and has been editor of 12 proceedings volumes. His work includes some 170 research articles in refereed journals, 58 chapters and in extenso contributions to proceedings, two books on scientific typography in Spanish and essays for the general public.